Generalized Elsässer Energy Spectra of the Ion Cyclotron and Whistler Modes in Magnetohydrodynamic and Hall Magnetohydrodynamic Turbulence*)

Keisuke ARAKI and Hideaki MIURA[1)]

Okayama University of Science, Okayama 700-0005, Japan
[1)]*National Institute for Fusion Science, Toki 509-5292, Japan*

(Received 25 November 2014 / Accepted 18 February 2015)

Applying the generalized Elsasser variables (GEV) decomposition method [S. Galtier, J. Plasma Phys. **72**, 721 (2006)] and using a dissipation-scale adaptive, wavelet-like shell decomposition method and normalization by dissipation-scale characteristics [K. Araki and H. Miura, PFR **8**, 2401137 (2013)] to direct numerical simulation datasets, we analyzed the energy and transfer spectra of freely decaying, homogeneous, and isotropic turbulence of incompressible magnetohydrodynamic (MHD) and Hall MHD (HMHD) media. The GEV decomposition analysis directly confirmed the breaking of chiral symmetry and the dominance of the right-handed polarized (whistler) modes over the left-handed polarized (ion cyclotron) modes, which Meyrand and Galtier had found using indirect parameters [R. Meyrand and S. Galtier, PRL **109**, 194501 (2012)].

Keywords: Hall magnetohydrodynamics, fully developed turbulence, generalized Elsässer variables

DOI: 10.1585/pfr.10.3401030

1. Introduction

Modeling of turbulent transport processes is regarded as an important key in the study of fusion plasmas in large torus devices. Hall magnetohydrodynamics (HMHD) is well known as a simple model of the large-scale motion of plasmas. As it contains the two-fluid effects, i.e., those of finite ion skin depth, it is expected to cover small-scale dynamics rather than the standard magnetohydrodynamic (MHD) models.

In our previous studies [1,2], we found self-similarity of the energy transfer process wherein the nonlinear interaction is gradually suppressed and the mutual interaction between the velocity and magnetic fields grows to compensate for the suppression. This phenomenon suggests that the coupling between the velocity and magnetic fields is crucial to the energy transfer process. The generalized Elsässer variables (GEV) decomposition, originated by Galtier [3], seems to provide a clue to the problem, because GEV naturally decompose the function space of the HMHD system according to its native linear wave modes. In the present study, we apply the decomposition to direct numerical simulation datasets.

2. Basic Equations

The time development of an incompressible HMHD plasma motion is determined by the following equation:

$$\partial_t \vec{\boldsymbol{Z}} = \vec{\boldsymbol{Q}}(\vec{\boldsymbol{Z}}, \vec{\boldsymbol{Z}}) + \hat{D}\vec{\boldsymbol{Z}}, \tag{1}$$

where $\vec{\boldsymbol{Z}} = {}^t(\boldsymbol{u}\ \boldsymbol{b})$ is a pair of velocity and magnetic fields; hereafter, called $\vec{\boldsymbol{Z}}$-variables. The quadratic term $\vec{\boldsymbol{Q}}$ and the dissipation term $\hat{D}\vec{\boldsymbol{Z}}$ are defined by:

$$\vec{\boldsymbol{Q}}(\vec{\boldsymbol{Z}}_1, \vec{\boldsymbol{Z}}_2) = \begin{pmatrix} \boldsymbol{u}_1 \times (\nabla \times \boldsymbol{u}_2) + (\nabla \times \boldsymbol{b}_1) \times \boldsymbol{b}_2 - \nabla P \\ \nabla \times ((\boldsymbol{u}_1 - \alpha(\nabla \times \boldsymbol{b}_1)) \times \boldsymbol{b}_2) \end{pmatrix}, \tag{2}$$

$$\hat{D}\vec{\boldsymbol{Z}} = {}^t(\nu\triangle\boldsymbol{u}\ \eta\triangle\boldsymbol{b}), \tag{3}$$

where P, ν, α, and η are generalized pressure, kinematic viscosity, the parameter specifying the relative strength of the Hall term effect, and resistivity, respectively. The operator $\vec{\boldsymbol{Q}}$, which has its origin in the variational formulation of a dissipationless HMHD system [4], is defined by the following formula:

$$\langle \vec{\boldsymbol{Z}}_1 \big| \vec{\boldsymbol{Q}}(\vec{\boldsymbol{Z}}_2, \vec{\boldsymbol{Z}}_3) \rangle := \langle \vec{\boldsymbol{Z}}_3 \big| \{\vec{\boldsymbol{Z}}_1, \vec{\boldsymbol{Z}}_2\} \rangle, \tag{4}$$

where $\langle * \,|\, * \rangle$, $\{*,*\}$ are the inner products of $\vec{\boldsymbol{Z}}$-variables defined by

$$\langle \vec{\boldsymbol{Z}}_1 \big| \vec{\boldsymbol{Z}}_2 \rangle := \int (\boldsymbol{u}_1 \cdot \boldsymbol{u}_2 + \boldsymbol{b}_1 \cdot \boldsymbol{b}_2)\ \mathrm{d}^3\vec{x}, \tag{5}$$

and the Lie bracket whose definition is also given in [4].

3. Generalized Elsässer Variables

The GEV that orthogonally decompose the function space of a pair of velocity and magnetic fields ($\boldsymbol{u}$, $\boldsymbol{b}$) are given by the following formulas [3,4]:

$$\vec{\boldsymbol{Z}}^{s_k}_{\sigma_k}(\vec{k}) = \widehat{Z}^{s_k}_{\sigma_k}(\vec{k}) \begin{pmatrix} \boldsymbol{\phi}_{\sigma_k}(\vec{k}) \\ \lambda^{s_k}_{\sigma_k}(\vec{k}) \boldsymbol{\phi}_{\sigma_k}(\vec{k}) \end{pmatrix}, \tag{6}$$

author's e-mail: araki@are.ous.ac.jp

*) This article is based on the presentation at the 24th International Toki Conference (ITC24).

$$\widehat{Z}^{s_k}_{\sigma_k}(\vec{k}) = \frac{\hat{u}_{\sigma_k}(\vec{k}) + \lambda^{s_k}_{\sigma_k}(\vec{k})\,\hat{b}_{\sigma_k}(\vec{k})}{1+\lambda^{s_k}_{\sigma_k}(\vec{k})^2}, \tag{7}$$

where $\boldsymbol{\phi}_{\sigma_k}(\vec{k})$, $\lambda^{s_k}_{\sigma_k}(\vec{k})$, $\hat{u}_{\sigma_k}(\vec{k})$, and $\hat{b}_{\sigma_k}(\vec{k})$ are the complex helical waves (CHW) [5,6], the eigenvalues of the operator $\hat{M}$ given below, and the Fourier coefficients of the velocity and magnetic fields, respectively, and are given as follows:

$$\boldsymbol{\phi}_{\sigma_k}(\vec{k}) = 2^{-1/2}(\boldsymbol{e}_\theta(\vec{k}) + i\sigma_k \boldsymbol{e}_\phi(\vec{k}))\exp(2\pi i\vec{k}\cdot\vec{x}), \tag{8}$$

$$\lambda^{s_k}_{\sigma_k}(\vec{k}) = \sigma_k\left(s_k\sqrt{(\pi\alpha|\vec{k}|)^2+1} - \pi\alpha|\vec{k}|\right), \tag{9}$$

$$\hat{f}_{\sigma_k}(\vec{k}) = \int \boldsymbol{f}(\vec{x},t)\cdot\overline{\boldsymbol{\phi}_{\sigma_k}(\vec{k})}\,\mathrm{d}^3\vec{x}, \qquad \text{for } \boldsymbol{f} = \boldsymbol{u},\ \boldsymbol{b}. \tag{10}$$

The symbols σ_k, s_k, $\boldsymbol{e}_\theta(\vec{k})$, and $\boldsymbol{e}_\phi(\vec{k})$ are helicity ($\sigma_k = \pm 1$), polarity ($s_k = \pm 1$), and unit vectors in the θ- and ϕ-directions of the spherical coordinate system in wavenumber space, respectively. Note that in the standard MHD, i.e., the limit $\alpha \to 0$ (where $\lambda^{s_k}_{\sigma_k}(\vec{k}) \to \sigma_k s_k$), GEV's orthogonality still remains.

The variables are derived as eigenfunctions of the linearized dissipationless HMHD equations given by:

$$\partial_t \boldsymbol{u} = \boldsymbol{B}_0\cdot\nabla\boldsymbol{b} - \nabla P_0, \tag{11}$$

$$\partial_t \boldsymbol{b} = \boldsymbol{B}_0\cdot\nabla(\boldsymbol{u} - \alpha(\nabla\times\boldsymbol{b})), \tag{12}$$

where $\boldsymbol{B}_0$ and P_0 are a uniform background magnetic field and generalized pressure, respectively. Using Fourier coefficients of the CHW expansion, we can write the equation in the operator matrix form

$$\frac{\partial}{\partial t}\begin{pmatrix}\hat{u}_{\sigma_k}(\vec{k})\\ \hat{b}_{\sigma_k}(\vec{k})\end{pmatrix} = 2\pi i B_0 k_\parallel \hat{M}\begin{pmatrix}\hat{u}_{\sigma_k}(\vec{k})\\ \hat{b}_{\sigma_k}(\vec{k})\end{pmatrix}, \tag{13}$$

where

$$\hat{M} = \begin{pmatrix} O & I\\ I & -\alpha\nabla\times\end{pmatrix} = \begin{pmatrix} O & I\\ I & -2\pi\alpha\sigma_k|\vec{k}|\end{pmatrix}. \tag{14}$$

In the limit $\alpha \to 0$, the eigenfunctions converge to the Alfvén waves of standard MHD systems.

A GEV function has two field-twisting direction parameters: σ and s. Parameter σ, which we call "helicity" hereafter, determines the spatial variation of the rotation direction of the snapshot of the velocity and magnetic fields. When $\sigma = +1$ (resp. $= -1$), the direction of the snapshot vector field rotates in the left-(right-)handed direction as the spatial position moves in the wavenumber vector direction. However, parameter s designates the time development of the rotation direction of the velocity and magnetic fields when the uniform background magnetic field $\boldsymbol{B}_0$ exists. For $s = +1$ (resp. $= -1$), the field vector temporally rotates in the left-(right-)handed direction with respect to the wavenumber vector; hereafter, called "polarity."

The eigenfunctions with polarity $s_k = +1$ express the ion cyclotron waves:

$$\vec{\boldsymbol{Z}}^+_\pm(\vec{k}) = \frac{\lambda\hat{u}_\pm(\vec{k}) \pm \hat{b}_\pm(\vec{k})}{1+\lambda^2}\begin{pmatrix}\lambda\boldsymbol{\phi}_\pm(\vec{k})\\ \pm\boldsymbol{\phi}_\pm(\vec{k})\end{pmatrix}, \tag{15}$$

Table 1 Differences between the decompositions of HMHD modes.

decomposition	combinations of GEV
ion cyclotron/whistler	$\{\widehat{Z}^+_+, \widehat{Z}^+_-\}$, $\{\widehat{Z}^-_+, \widehat{Z}^-_-\}$
conventional Elsässer (in $\alpha \to 0$ limit)	$\{\widehat{Z}^+_+, \widehat{Z}^-_-\}$, $\{\widehat{Z}^-_+, \widehat{Z}^+_-\}$
complex helicity [7]	$\{\widehat{Z}^+_+, \widehat{Z}^-_+\}$, $\{\widehat{Z}^+_-, \widehat{Z}^-_-\}$

where $\lambda = \lambda^-_-(\vec{k}) = ((\pi\alpha|\vec{k}|)^2+1)^{1/2} + \pi\alpha|\vec{k}|$ is the largest eigenvalue for an assigned $\vec{k}$ and $\lambda^{s_k}_{\sigma_k}(\vec{k}) = \sigma_k s_k \lambda^{-s_k}$. As λ is an increasing function of the wavenumber modulus $|\vec{k}|$, the modulus of the phase velocity of the left-handed modes $B_0 k_\parallel/\lambda$ decreases as the wavenumber increases. However, the eigenfunctions with $s_k = -1$ express the whistler waves:

$$\vec{\boldsymbol{Z}}^-_\pm(\vec{k}) = \frac{\lambda\hat{b}_\pm(\vec{k}) \mp \hat{u}_\pm(\vec{k})}{1+\lambda^2}\begin{pmatrix}\mp\boldsymbol{\phi}_\pm(\vec{k})\\ \lambda\boldsymbol{\phi}_\pm(\vec{k})\end{pmatrix}. \tag{16}$$

They are right-handed polarized and their phase velocity is an increasing function of the wavenumber.

An important advantage of the introduction of GEV is that the basic equations are given by the following simple form in the limit $\nu, \eta \to 0$ [3,4]:

$$\partial_t\overline{\widehat{Z}^{s_k}_{\sigma_k}(\vec{k})} = \sum_{\vec{p},\sigma_p,s_p}\sum_{\vec{q},\sigma_q,s_q}\frac{\left(\!\left(^{s_k}_{\sigma_k}\vec{k}\middle|^{s_p}_{\sigma_p}\vec{p}\middle|^{s_q}_{\sigma_q}\vec{q}\right)\!\right)\lambda^{-s_q}_{\sigma_q}(\vec{q})}{\lambda^{s_k}_{\sigma_k}(\vec{k})^2+1} \times \widehat{Z}^{s_p}_{\sigma_p}(\vec{p})\,\widehat{Z}^{s_q}_{\sigma_q}(\vec{q}), \tag{17}$$

where an overline denotes the complex conjugate and the symbol $\left(\!\left(^{s_k}_{\sigma_k}\vec{k}\middle|^{s_p}_{\sigma_p}\vec{p}\middle|^{s_q}_{\sigma_q}\vec{q}\right)\!\right)$ is defined as follows:

$$\left(\!\left(^{s_k}_{\sigma_k}\vec{k}\middle|^{s_p}_{\sigma_p}\vec{p}\middle|^{s_q}_{\sigma_q}\vec{q}\right)\!\right) := \alpha^{-1}\left(\left(\lambda^{s_k}_{\sigma_k}(\vec{k})\lambda^{s_p}_{\sigma_p}(\vec{p})\lambda^{s_q}_{\sigma_q}(\vec{q})\right)^2 - 1\right) \times \int_{\vec{x}\in M}\boldsymbol{\phi}_{\sigma_k}(\vec{k})\cdot\left(\boldsymbol{\phi}_{\sigma_p}(\vec{p})\times\boldsymbol{\phi}_{\sigma_q}(\vec{q})\right)\mathrm{d}^3\vec{x}. \tag{18}$$

In the following, we consider the decomposition with respect to polarity s using the following notations

$$\vec{\boldsymbol{Z}}^+ := \sum_{\vec{k},\sigma_k}\vec{\boldsymbol{Z}}^+_{\sigma_k}(\vec{k}), \qquad \vec{\boldsymbol{Z}}^- := \sum_{\vec{k},\sigma_k}\vec{\boldsymbol{Z}}^-_{\sigma_k}(\vec{k}), \tag{19}$$

and we call them the "ion cyclotron mode" and "whistler mode," even when the Hall term parameter α vanishes.

Note that in the limit $\alpha \to 0$, the relations between the conventional Elsässer variables and GEV are given as follows:

$$z_+ := \boldsymbol{u} + \boldsymbol{b} = \widehat{Z}^+_+(\vec{k})\,\boldsymbol{\phi}_+(\vec{k}) + \widehat{Z}^-_-(\vec{k})\,\boldsymbol{\phi}_-(\vec{k}), \tag{20}$$

$$z_- := \boldsymbol{u} - \boldsymbol{b} = \widehat{Z}^-_+(\vec{k})\,\boldsymbol{\phi}_+(\vec{k}) + \widehat{Z}^+_-(\vec{k})\,\boldsymbol{\phi}_-(\vec{k}). \tag{21}$$

Thus, each of the conventional Elsässer variables does not directly correspond to the linear wave branch that connects with the ion cyclotron or whistler mode. Possible combinations of the GEV are summalized in Table 1.

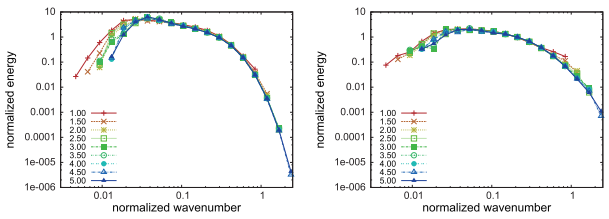

Fig. 1 Time series of the normalized and shell-averaged energy spectra of the GEV decomposed modes for the HMHD case ($\alpha = 0.05$). Left: the ion cyclotron modes, right: whistler modes. Change in line colors from red to blue denotes time development of spectra.

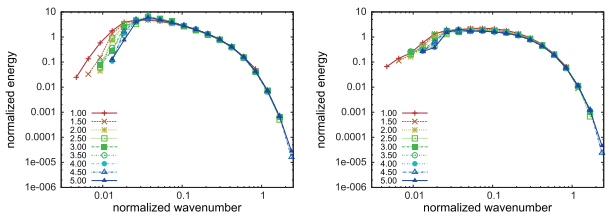

Fig. 2 Time series of the normalized and shell-averaged energy spectra of the GEV decomposed modes for the MHD case ($\alpha = 0$). Shown are the mode branch of Alfvén waves connected to (left) the ion cyclotron modes and (right) the whistler modes. The color legend is the same as that in Fig. 1.

4. Time Development of Energy and Transfer Function Spectra

In this study, we used the same snapshot data as those used in Refs. [1] and [2]. The amplitudes and wavenumbers of the various spectra are normalized using the dissipation rate of magnetic energy $\epsilon_B(t) = \eta \int |\nabla \times \boldsymbol{b}|^2 \mathrm{d}^3\vec{x}$ at each snapshot. To calculate the shell-averaged spectral quantities, the wavenumber space is divided into the spherical shell band with wavenumber ranges $k_\eta(t)/2^{(j+1)/2} < k < k_\eta(t)/2^{j/2}$, where $k_\eta(t) = (\epsilon_B(t)/\eta^3)^{1/4}$ and j is a shell index, hereafter. The combination of the normalization and shell decomposition methods has been demonstrated to clearly capture the self-similarity features of freely decaying turbulence [1].

In this study, we focused our attention on the comparison between an analysis of the standard $\boldsymbol{u}$, $\boldsymbol{b}$ variables and that based on the GEV decomposed modes. Numerical decomposition and reconstruction programs are coded according to the Eqs. (15) and (16).

In Figs. 1 and 2, we plotted the time series of the normalized and shell-averaged energy spectra of the ion cyclotron and whistler modes, which are defined by $E_j^{(I)} = \frac{1}{2}\langle \vec{\boldsymbol{Z}}_j^+ | \vec{\boldsymbol{Z}}_j^+ \rangle$, and $E_j^{(W)} := \frac{1}{2}\langle \vec{\boldsymbol{Z}}_j^- | \vec{\boldsymbol{Z}}_j^- \rangle$, respectively.

As can be seen from Eqs. (15) and (16), because the velocity component of the ion cyclotron mode $\vec{\boldsymbol{Z}}^+$ is weighted by λ for both the Fourier coefficient and the base function and because the value of λ is an increasing function of the wavenumber modulus, the functional form of their energy spectrum is expected to approach that of the kinetic energy spectrum as the modulus of wavenumber increases. An analogous tendency is expected between the whistler mode $\vec{\boldsymbol{Z}}^-$ and the magnetic energy spectra. In Fig. 1 we show the spectra for the case where $\alpha = 0.05$. It can be verified by comparison with the spectra shown in Fig. 3 of Ref. [1], that their functional forms obey our expectation for higher wavenumber ranges ($k \gtrsim 0.3k_\eta$).

This tendency has an important implication. As is shown in Ref. [8], the dominance of the whistler mode energies implies the spontaneous breaking of chiral symmetry of small-scale motions. Although the method to extract the mirror symmetry of fields is different, our results support the results presented in Ref. [8].

For intermediate and lower wavenumber ranges ($k \lesssim 0.3k_\eta$), λ gradually approaches 1 as the wavenumber decreases, i.e., the weights of the velocity and magnetic fields become closer irrespective of polarity s; therefore it is expected that the functional profile of the GEV mode energies becomes some "averaged" form. However, numerical results show tendencies whereby the functional forms of the ion cyclotron (whistler) mode energy spectra have profiles close to those of the magnetic (resp. kinetic) energy.

For the standard MHD case ($\alpha = 0$), we also compared the kinetic/magnetic and the GEV energy spectra. The functional profiles of the GEV energy spectra are expected to fall in an "averaged profile" of the kinetic and magnetic energy spectra, because $\lambda \to 1$ for $\alpha \to 0$, i.e., the contributions of the velocity and magnetic fields to the amplitudes of the GEV modes (see Eqs. (15) and (16)) become the same.

Comparing Fig. 2 with Fig. 3 of Ref. [1], we found that the amplitudes and functional forms of the ion cyclotron (whistler) mode energy spectra are very close to the magnetic (resp. kinetic) spectra. Although this result is very interesting, elucidation of its implications will be discussed in a future study.

We considered the GEV representation of the energy transfer functions. In each panel of Figs. 3 and 4, we show the energy transfer function spectra corresponding to those in Figs. 1 and 2. The transfer of the kinetic, magnetic, ion cyclotron mode, and whistler mode energies to the j-th shell are given by

$$T_j^{(K)} := \langle {}^t(\boldsymbol{u}_j\ \boldsymbol{0}) | \vec{\boldsymbol{Q}}(\vec{\boldsymbol{Z}}, \vec{\boldsymbol{Z}}) \rangle,$$
$$T_j^{(M)} := \langle {}^t(\boldsymbol{0}\ \boldsymbol{b}_j) | \vec{\boldsymbol{Q}}(\vec{\boldsymbol{Z}}, \vec{\boldsymbol{Z}}) \rangle,$$
$$T_j^{(I)} := \langle \vec{\boldsymbol{Z}}_j^+ | \vec{\boldsymbol{Q}}(\vec{\boldsymbol{Z}}, \vec{\boldsymbol{Z}}) \rangle,$$
$$T_j^{(W)} := \langle \vec{\boldsymbol{Z}}_j^- | \vec{\boldsymbol{Q}}(\vec{\boldsymbol{Z}}, \vec{\boldsymbol{Z}}) \rangle,$$

respectively.

In Fig. 3, the transfer functions for the HMHD case are shown. The transfer function spectra of the ion cyclotron (resp. whistler) mode have close functional form to those of the kinetic (resp. magnetic) energy for interme-

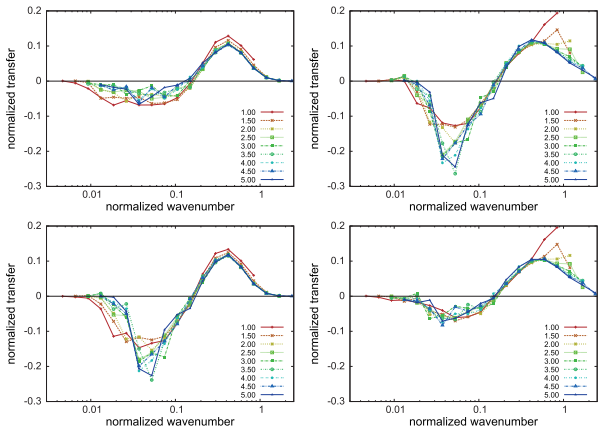

Fig. 3 Time series of the normalized and shell-averaged energy transfer spectra of the $\boldsymbol{u}$, $\boldsymbol{b}$ variables (top) and the GEV (bottom) for the HMHD case ($\alpha = 0.05$). Top: kinetic (left) and magnetic (right) energy transfer spectra. Bottom: ion cyclotron mode (left) and whistler mode (right) energy transfer spectra.

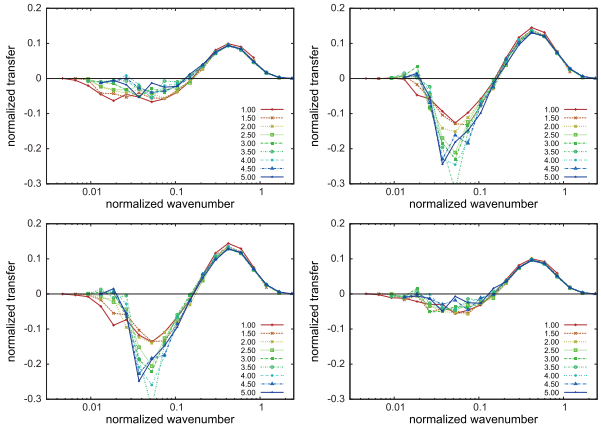

Fig. 4 Time series of the shell-averaged energy transfer spectra for the MHD case ($\alpha = 0$). The quantity shown in each panel and the changes in line colors are the same as in Fig. 3.

diate and higher wavenumber ranges ($k \gtrsim 0.1k_\eta$) and those of the magnetic (resp. kinetic) energy for lower wavenumber ranges ($k \lesssim 0.1k_\eta$). This "switching" tendency corresponds to those found for the energy spectra. However, the tendency of the energy transfer function profiles for the standard MHD case ($\alpha = 0$) seems to reflect that of the energy spectra, i.e., the pair of kinetic and whistler mode energy transfers and that of the magnetic and ion cyclotron modes have similar profiles.

5. Discussion

In this paper, we reviewed the GEV as an orthogonal basis of the function space of the HMHD system and its relation to the conventional Elsässer variables for the MHD system from a mathematical viewpoint. The GEV analysis provided the decomposition with respect to the chiral (or mirror) symmetry of linear wave modes. Spontaneous breaking of the chiral symmetry of the plasma velocity and magnetic fields was clearly captured in the difference of the energy spectra between the ion cyclotron and whistler modes. In particular, the disparity became significant at higher wavenumber regions.

It is well known that the issues of spontaneous breaking of isotropy and mirror symmetry in fully developed turbulence in plasmas are important for understanding their dynamics (e.g., Refs. [9, 10]). In the present study, we investigated homogeneous, isotropic turbulence and focused our attention on the breaking of mirror symmetry as a starting point of the analysis, and therefore, some issues remain for future works.

In terms of the statistical anisotropy, which is mainly due to the existence of uniform background magnetic fields, it was clear from the derivation process of the GEV that they retain their orthogonality, even when a uniform background magnetic field exists.

The ideally conserved quantities are known to affect the dynamics, even in the dissipative processes. For the MHD system, Perez and Boldyrev numerically confirmed that the value of cross helicity strongly affects its dynamics [9]. It is well known that the HMHD dynamics conserve the magnetic and hybrid (or generalized) helicities [11,12]. Recently, we demonstrated that the modified cross helicity, which is defined by the difference between the hybrid and magnetic helicities, is naturally derived from the GEV representation of the HMHD system Eq. (18). Therefore, the GEV decomposition of the HMHD system is expected to provide a powerful tool to analyze how these helicities affect the energy transfer process.

This study was performed under the auspices of the NIFS Collaboration Research Program (NIFS13KNSS044) and KAKENHI (Grant-in-Aid for Scientific Research(C)) 23540583.

[1] K. Araki and H. Miura, Plasma Fusion Res. **8**, 2401137 (2013).
[2] K. Araki and H. Miura, Plasma Fusion Res. **9**, 3401073 (2014).
[3] S. Galtier, J. Plasma Phys. **72**, 721 (2006).
[4] K. Araki, to appear in J. Phys. A: Math. Theor. (2015).
[5] M. Lesieur, *Turbulence in Fluids: Third Revised and Enlarged Edition* (Kluwer, Dortrecht, 1997).
[6] F. Waleffe, Phys. Fluids **A 4**, 350 (1992).
[7] S. Galtier, J. Fluid Mech. **757**, 114 (2014).
[8] R. Meyrand and S. Galtier, Phys. Rev. Lett. **109**, 194501 (2012).
[9] J.C. Perez and S. Boldyrev, Phys. Rev. Lett. **102**, 025003 (2009).
[10] S. Boldyrev *et al.*, Astrophys. J. Lett. **741**, L19 (2011).
[11] L. Turner, IEEE Trans. Plasma Sci. **14**, 849 (1986).
[12] S.M. Mahajan and Z. Yoshida, Phys. Rev. Lett. **81**, 4863 (1998).